PAPER

Check for updates

Self-powered impact sensors based on electrospun acrylonitrile butadiene styrene triboelectric nanogenerators for wearable helmet applications

Mathew Sunil,[a,b] E. J. Jelmy,[c] Rinku Mariam Thomas,[d] K. J. Saji[b,c] and Honey John ✱[a,c]

The recent developments in the self-powered sensing technologies have immensely contributed to wearable energy harvesting systems for safety applications. This study presents the first elucidation of incorporating electrospun acrylonitrile butadiene styrene (ABS) nanofiber-based triboelectric nanogenerators (TENGs) into a smart wearable helmet for real-time impact detection and wireless alert transmission. The neat ABS nanofibers produced after the 4 h electrospinning process showed the highest triboelectric output when compared to the 2 h, 6 h, and 8 h electrospun samples with an open circuit voltage (V_{oc}) of 48.1 V, a short circuit current (I_{sc}) of 3.1 μA, and a transferred charge of 13.4 nC. The effect of the impact force and contact frequency was systematically studied and the optimal efficiency was confirmed at 5 N and 10 Hz. The 1 cm² TENG device achieved a peak power density of 903 mW m⁻² at a 70 MΩ load resistance and cycling stability over 4000 cycles showed its strong potential for energy harvesting and sensing applications. On simple hand tapping, the device exhibited an output of 200 V and 12 μA, which was used to charge a commercially available capacitor. A smart wearable helmet was designed for real-time impact detection by strategically placing the fabricated TENG units in the helmet at different positions. The signals generated from the helmet were processed using a microcontroller and transmitted through a Bluetooth module ensuring rapid detection and user notification.

Introduction

The development of Internet of Things (IoTs) and sensor technology has accelerated the growth of sensor networks enhancing modern industries that rely on health monitoring. In this network, integrating multiple wearable sensors for individuals allow real-time human–machine interactions, enabling the transmission of on-site data regarding the individual health status. These flexible devices can be connected to skin or embedded in clothing, footwear, gloves, helmets, etc.[1–4] With its real-time monitoring and communication capabilities, wearable technology improves user protection and is vital to modern safety gear, particularly in smart helmets. Smart

helmets facilitate hands-free navigation and communication, keeping users connected while allowing them to stay focused on their work. For users in various industries, such as sports, mining, and construction, wearable technology in smart helmets thus improves situational awareness and efficiency in addition to safety.[5,6]

Wearable electronics face limitations due to bulky, rigid batteries with finite lifespans and maintenance needs. Harvesting energy from mechanical vibrations and body movements offers a promising alternative. Triboelectric nanogenerators (TENGs) efficiently convert environmental and body motion into power and they can provide a viable solution for self-powered wearable electronics.[7,8] TENGs operate through the principles of contact-induced charging and electrostatic induction.[9] When two materials are made to come in contact and then separated, they exchange electrons based on their differing electron affinities.[10,11] This led to a material attaining a positive charge and the opposite contact material attaining a negative charge. As the materials move apart, an electric field forms between them, generating a voltage difference. When a circuit is connected, electrons flow, producing an electrical current that can be harnessed for our energy needs. For TENG

*a*Department of Polymer Science and Rubber Technology, Cochin University of Science and Technology, Cochin 22, Kerala, India. E-mail: honey@cusat.ac.in
*b*International School of Photonics, Cochin University of Science and Technology, Cochin 22, Kerala, India
*c*Inter University Centre for Nanomaterials and Devices, Cochin University of Science and Technology, Cochin 22, Kerala, India
*d*Department of Mathematics and Natural Sciences, School of Arts and Science, American University of Ras Al Khaimah, Ras Al Khaimah, United Arab Emirates

devices to function efficiently in energy harvesting and sensing, selecting suitable materials is crucial. The triboelectric series classifies materials according to their ability to donate or accept electrons during interactions.[12] Materials at opposite ends of the series exhibit strong electron affinity differences, enhancing charge transfer for TENG applications. Ideal TENG materials should have surface roughness for better contact and charge movement, high durability for repeated use, flexibility for diverse designs, environmental stability for reliability, and cost-effectiveness for commercial viability.[13–15]

A lightweight TENG for wearable safety gear can be developed using polymer-based materials that possess the aforementioned properties. A pressure sensor based on porous PDMS polymers for sports applications such as in determining appropriate fit of the helmets was reported by Masihi *et al.*[16] A similar work was reported in which a piezoresistive smart safety helmet was developed combining a microporous PDMS elastomer and carbon nanoparticles.[4] This sensor measures the pressure between the skin and the head band of the safety helmet and evaluates the appropriate alignment and fit of the safety helmet. The smart helmet also helps in identifying the areas of impact within the head. Acrylonitrile butadiene styrene (ABS) is a terpolymer containing conjugated double bonds with π electrons for electron donation and delocalized electrons.[17] The localized π electrons enhance the charge contributing ability of the material and the delocalization helps in reducing the charge dissipation by improving the charge retention capability. Being a tribopositive polymer, ABS significantly boosts the triboelectric charge transfer efficiency.[18] The exceptional stability and mechanical strength make it an ideal material for protective gear, such as helmets, knee and elbow guards, shin guards, *etc.*, ensuring reliability and safety in demanding environments.[19] At the same time, the long-term impact of ABS on the environment is an important consideration. This concern is addressed by minimising the amount of ABS used for this work, which is suitable for long term, durable safety devices rather than disposable application. Additionally, ABS is a recyclable thermoplastic, which can be recovered and reused. In future studies, bio-based ABS alternatives can be explored to further improve the sustainability of the devices. Patra *et al.* fabricated a TENG unit from waste materials consisting of a blend of ABS and polyethylene terephthalate (PET).[20] With a device area of 2.5 cm × 2.5 cm, an output of 124.8 V and 5.5 μA cm^{-2} was achieved under an applied impact force of 40 N at a frequency of 4 Hz. The ABS TENG with a compact size, low-cost fabrication, and lightweight design can function both as a mechanical energy harvesting and a self-powered sensing system. Even though ABS is used in compact TENG devices, a majority of the studies are limited to bulk films or blends, while, the exploration of electrospun ABS as an active tribomaterial remains limited. Electrospinning offers a scalable and adaptable method for fabricating high-performance TENGs using ABS nanofibers.[21,22] Unlike flat drop-cast, spin-coated, or microstructured films, electrospun ABS nanofibers provide an uneven, aligned surface that enhances charge transfer

efficiency.[23] This unique morphology improves triboelectric performance by optimizing the surface texture and material properties, making electrospinning a promising strategy for TENG device fabrication.[24]

To the best of our knowledge, this study presents an electrospun ABS nanofiber-based TENG integrated into a smart helmet for impact sensing applications. The nanofibers fabricated are optimized for various parameters to obtain a robust and durable ABS-based TENG capable of generating a power density of 903 mW m^{-2} under an external load resistance of 70 MΩ, with a contact area of 1 cm × 1 cm. The study primarily focusses on the refinement of the electrospinning parameters to achieve the maximum triboelectric output from ABS nanofibers and analysis to elucidate the correlation between the fiber's structure and the energy generated. A triboelectric smart helmet integrated with an electrospun ABS TENG was developed to establish a self-powered system for real-time impact sensing, enabling rapid safety predictions for all types of riders. The smart helmet showed in this study holds significant potential for intelligent riding gear, sports protection, and other shock-absorbing applications.

Experimental

Preparation of ABS nanofibers by electrospinning

ABS granules were dissolved in *N,N*-dimethylformamide (DMF) to prepare a 37 wt% ABS solution. This solution was then loaded into a 10 ml syringe equipped with a steel needle with an inner diameter of 800 μm. During the electrospinning process, the solution was dispensed at a controlled flow rate of 750 μl h^{-1} under an applied voltage of 27 kV. The needle tip was maintained at a fixed distance of 15 cm from the collector to ensure consistent fiber deposition. A schematic illustration of the preparation of the nanofiber mat is shown in Fig. 1. The electrospun nanofibers were collected on aluminium foil, which facilitated easy extraction for further processing.

To optimize the triboelectric performance, concentrations of ABS and spinning durations were systematically varied. The electrospinning parameters, including the applied voltage, needle-to-collector distance, flow rate, and ambient temperature, were kept constant throughout the experiments. The spinning duration was varied between 2 and 8 hours to assess its influence on the thickness of the electrospun fiber mat on TENG performances.
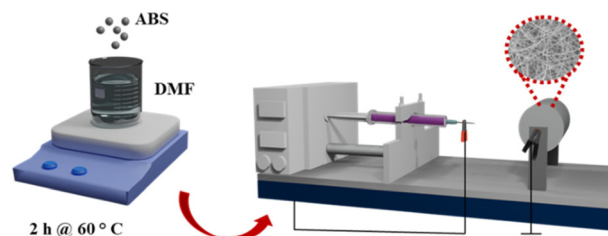

Fig. 1 Preparation of the ABS nanofiber mat.

Construction of a TENG and triboelectric measurements

A customized apparatus was employed to facilitate the controlled contact and separation of the triboelectric materials, enabling precise adjustment of both frequency (1 Hz to 10 Hz) and applied force (1 N to 10 N). A TENG unit with a size of 1 cm × 1 cm was fabricated with ABS as the positive triboelectric material and fluorinated ethylene propylene (FEP) as the negative triboelectric material.

The triboelectric materials were then affixed to copper electrodes using adhesive tape and these electrode-material assemblies were mounted onto polymeric substrates to maintain structural stability during operation. Electrical leads from the top and bottom electrodes were connected to an electrometer, enabling the TENG output measurement during the continuous contact–separation cycles of the triboelectric layers. To minimize the influence of environmental variability on TENG performance, all measurements were conducted within a controlled humidity range of 46% to 48%.

Development of the TENG device for impact sensing applications

Circular TENG modules with a 3 cm diameter of effective contact area was fabricated for the impact sensing application. The top electrode with FEP as the contact material and the bottom electrode with ABS as the contact material were securely attached to a PET substrate using double side tape. Copper wires connected to the electrodes acted as electrical leads and, durable rubber substrates were employed as separators between the PET layers. To optimize the sensing and energy harvesting applications, TENG units were strategically positioned on three sides of the helmet – top, left and right. To send alert notifications, the wires were attached to the microcontroller unit, which processes the analogue signals received and triggers the Bluetooth module to send the alert signal to the mobile devices.

Characterization of the electrospun samples

Different analytical methods were used for the structural and morphological characterization of the electrospun samples. The X-ray diffractogram of the electrospun samples was analyzed using a Bruker D8 advance system, employing Cu Kα1 radiation at a wavelength of 1.5418 Å. Attenuated Total Reflectance (ATR) of the samples was recorded using a Fourier Transform Infrared (FT-IR) spectrometer (Thermo Nicolet iS50) over a spectral range of 4000 cm^{-1} to 100 cm^{-1}. The wettability and contact angle measurements were performed using a contact angle goniometer (Rame Hart Model 290). A precisely engineered triboelectric setup was employed to control different forces (1 N–10 N) and frequencies (1 Hz–10 Hz). A Keithley electrometer 6517 B was employed to measure the short circuit current (I_{sc}), open circuit voltage (V_{oc}) and transferred charge.

Results and discussion

The electrospun nanofibers were characterized using FT-IR spectroscopy to analyse their structural composition as

detailed in the SI. The ability of ABS nanofiber mats as a triboelectric material for industrial applications was evaluated through a simplified structural configuration. Fig. 2 illustrates the fundamental design of the TENG module, fabricated for application as the sensor for the helmet. However, the initial analysis was done with a TENG of a 1 cm × 1 cm square designed to optimize the electrospinning parameters for achieving the highest possible triboelectric performance of the fabricated fibers. The top section comprises the substrate material, a copper electrode and FEP, whereas the bottom section consists of an ABS nanofiber mat, copper electrode and the substrate material. The top part is attached to a movable piston that continuously makes contact with and separates from the fixed bottom part, which remains stationary on the vertical side.

Additionally, Fig. 3 presents a detailed representation of the internal electron flow mechanism[25–27] during continuous contact and separation of tribomaterials. When FEP and ABS are made to come in contact with each other, charge transfer takes place on the surface of the materials. Since ABS is more tribopositive than FEP,[28] it gains positive charges, while FEP accumulates negative charges. When the materials are separated, an electric field develops across the electrodes, creating a potential difference that drives the electrons to move from the top electrode to the bottom electrode, generating an electric current. At the maximum separation of tribopairs, the potential difference diminishes to zero, halting the flow of charges. Conversely, when the top electrode is pressed against the bottom electrode, the induced electric field changes, resulting in another potential difference, producing an electric current pulse with reverse polarity. Consequently, the continuous contact and separation of the triboelectric materials lead to

Fig. 2 Schematic representation of the ABS-based TENG.
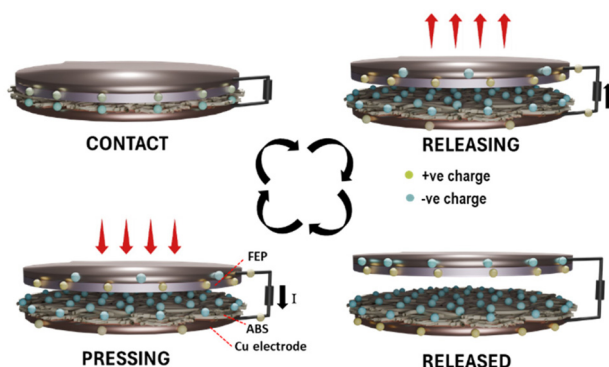
Fig. 3 Working principle of the vertical contact separation mode.

alternating positive and negative charge pulses in the system. The theoretical framework governing the electrical output characteristics of vertical contact and separation TENGs can be expressed mathematically. The V_{oc} and I_{sc} can be derived as follows:[27,29]

$$I_{sc} = \frac{\sigma_0 S v(t)}{(d_0 + x(t))^2},$$

$$V_{oc} = \frac{\sigma_0 x(t)}{\varepsilon_0},$$

where σ_0 is the surface charge density, which is dependent on the material composition and the effective area of contact between the two triboelectric surfaces. The variable $x(t)$ denotes the instantaneous distance between the contact materials during operation, while d_0 represents the thickness of the dielectric material. The term S corresponds to the contact surface, $v(t)$ represents the velocity of separation and ε_0 is the permittivity of free space.

For optimizing the electrospinning parameters, the ABS solution was spun for 2 h, 4 h, 6 h, and 8 h to study the influence of the thickness of the nanofiber mats on the triboelectric performance. The variation in the fiber diameter along with the distribution of fibers is observed from the FE-SEM micrographs, as shown in Fig. 4. The fiber with a 2 h electro-

spinning time exhibited a fiber diameter of ~400 nm, which increased to ~450 nm for the 4 h electrospun sample. On further increasing the electrospinning time beyond 4 hours, the diameter of the nanofibers increased to ~470 nm for 6 h and ~550 nm for the 8 h electrospun sample. The increase in fiber diameter was due to higher deposition density and secondary jet interactions during the extended electrospinning duration.[30,31] The 4 h electrospun sample exhibited the best balance of mat thickness and fiber structure. Furthermore, the structured stacking of layers, interwoven with minute air pockets, was instrumental in generating net surface charge through repeated interactions of contact and separation between them.[32] As the electrospinning time increased, the fibers became thicker (0.06 mm to 0.25 mm for 2 h to 8 h) due to a higher accumulation of polymer deposition. This initially enhanced the surface roughness and contact area with the counter triboelectric material, leading to an increase in charge generation.

Fig. 5(a), (b) and (c) illustrate the I_{sc}, V_{oc} and transferred charge of electrospun fibers prepared at different spinning durations. The triboelectric setup was operated at a consistent frequency of 10 Hz and an applied force of 5 N for a TENG unit of 1 cm × 1 cm. The nanofiber mats produced at 2 h, 4 h, 6 h, and 8 h spinning durations had a thickness of 0.06 mm, 0.128 mm, 0.186 mm, and 0.250 mm, respectively. As the spinning duration was increased from 2 h to 4 h, I_{sc} also increased
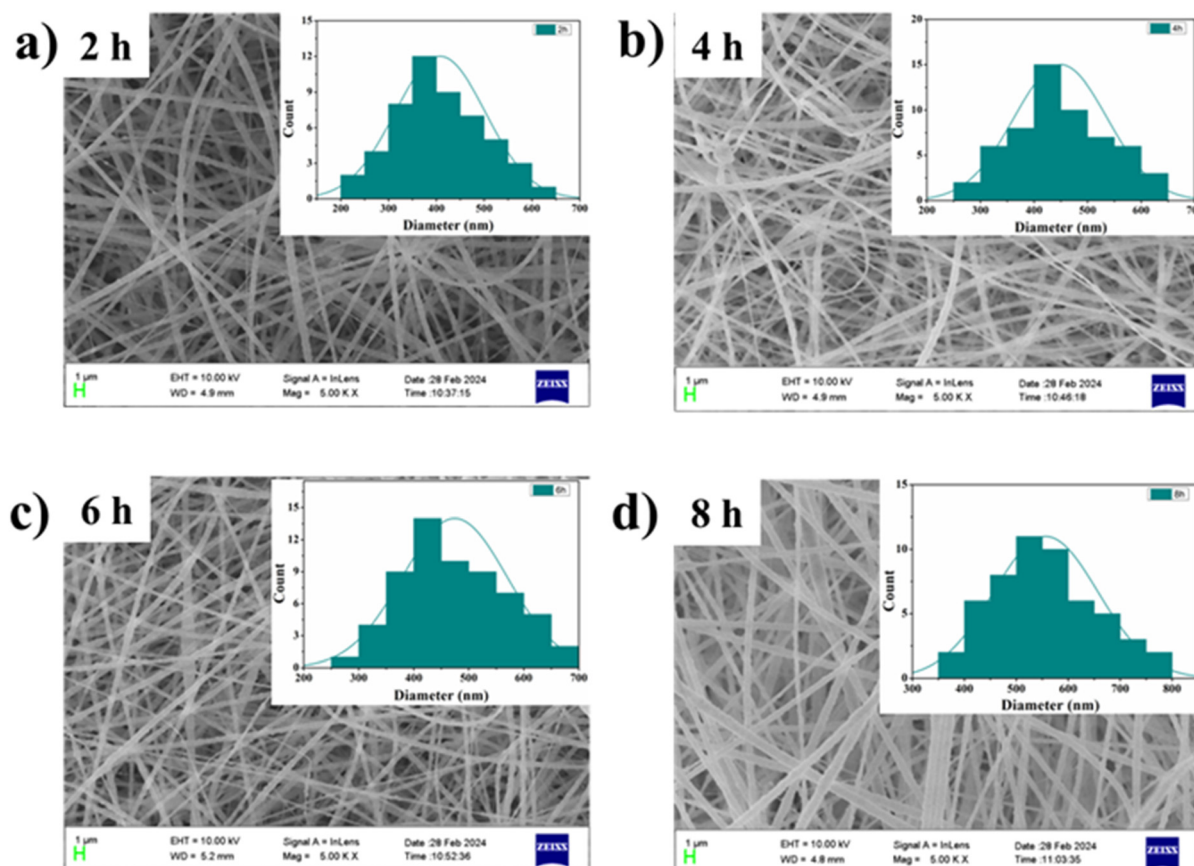

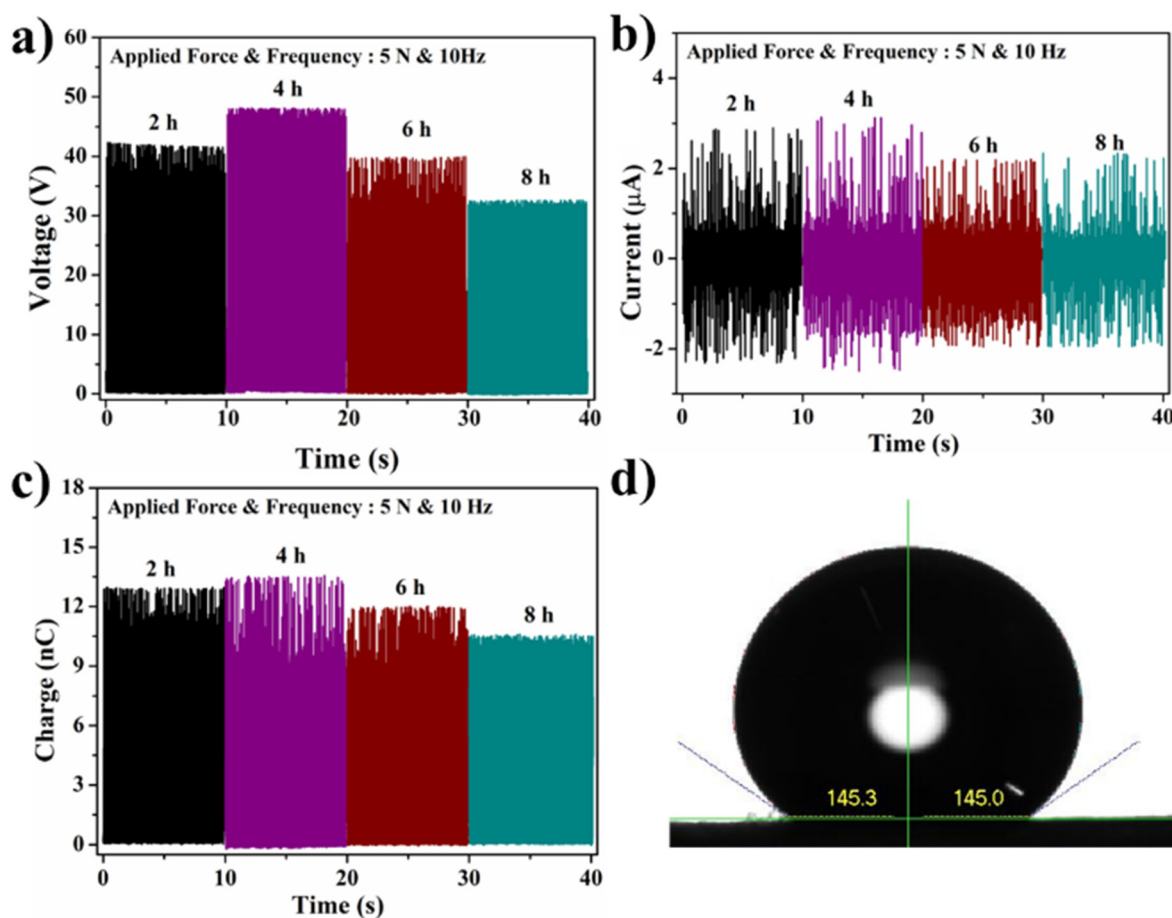**Fig. 4** FE-SEM micrographs of ABS electrospun for (a) 2 h, (b) 4 h, (c) 6 h and (d) 8 h.

Fig. 5 The triboelectric output of the electrospun ABS mat on varying the spinning time. (a) V_{oc}, (b) I_{sc}, (c) transferred charge and (d) contact angle measurement of the 4 h electrospun mat.

from 2.8 μA to 3.1 μA, V_{oc} from 42 V to 48.1 V, and transferred charge from 12.9 nC to 13.4 nC, followed by a gradual decline beyond 4 hours of spinning.

The decrease in triboelectric output for the 6 h and 8 h spun samples could be attributed to the thickness of the nanofiber mat and the increase in nanofiber diameter. The charges formed got dissipated due to the enhancement in the internal resistance caused by the increased mat thickness, leading to reduced surface charges. The charge transfer efficiency was affected by the weak electric field due to the thickness.[33] At the same time, the increased diameter profile for the nanofibers decreased the surface-to-volume ratio, lowering the charge density and diminishing the triboelectric effect.[34,35] This was supported by the surface profilometry studies shown in Fig. S2. For the 2 h sample, the roughness observed was within the range of ~8 nm, but for the 4 h sample, it was observed to be ~25 nm. This roughness decreased to ~13 nm and ~9 nm for the 6 h and 8 h electrospun samples.

The ABS nanofibers showed hydrophobic properties as confirmed by the contact angle measurements illustrated in Fig. 5(d). This hydrophobic nature plays a crucial role in minimizing the dissipation of frictional charges and improving

adaptability to fluctuations under ambient humidity conditions.[36] According to the Wenzel effect, an increase in surface roughness of the hydrophobic materials typically leads to a higher contact angle.[37] However, beyond a certain roughness threshold, the contact angle decreased as the droplet established a more effective contact with the surface. This was in agreement with the contact angle measurements of all the samples, as shown in Fig. S3. For the ABS nanofibers produced with a 2-hour electrospinning duration, the measured contact angle was 131.1°, which increased to 145.1° for 4 h. The contact angle then decreased to 124.7° and 121.3° for the 6 h and 8 h electrospun samples. The surface microstructures, combined with the thickness of the electrospun samples, exhibited a clear correlation with the increased surface charge density observed in the samples spun for 4 h. The influence of the applied force and operating frequency on the TENG output of the ABS nanofiber mat with a 4 h electrospinning duration was examined with TENG dimensions of 1 cm × 1 cm. The triboelectric output was measured with ABS as the tribopositive component and FEP as the tribonegative counterpart.

To investigate the impact of external force on the performance of TENGs, the applied force was systematically varied
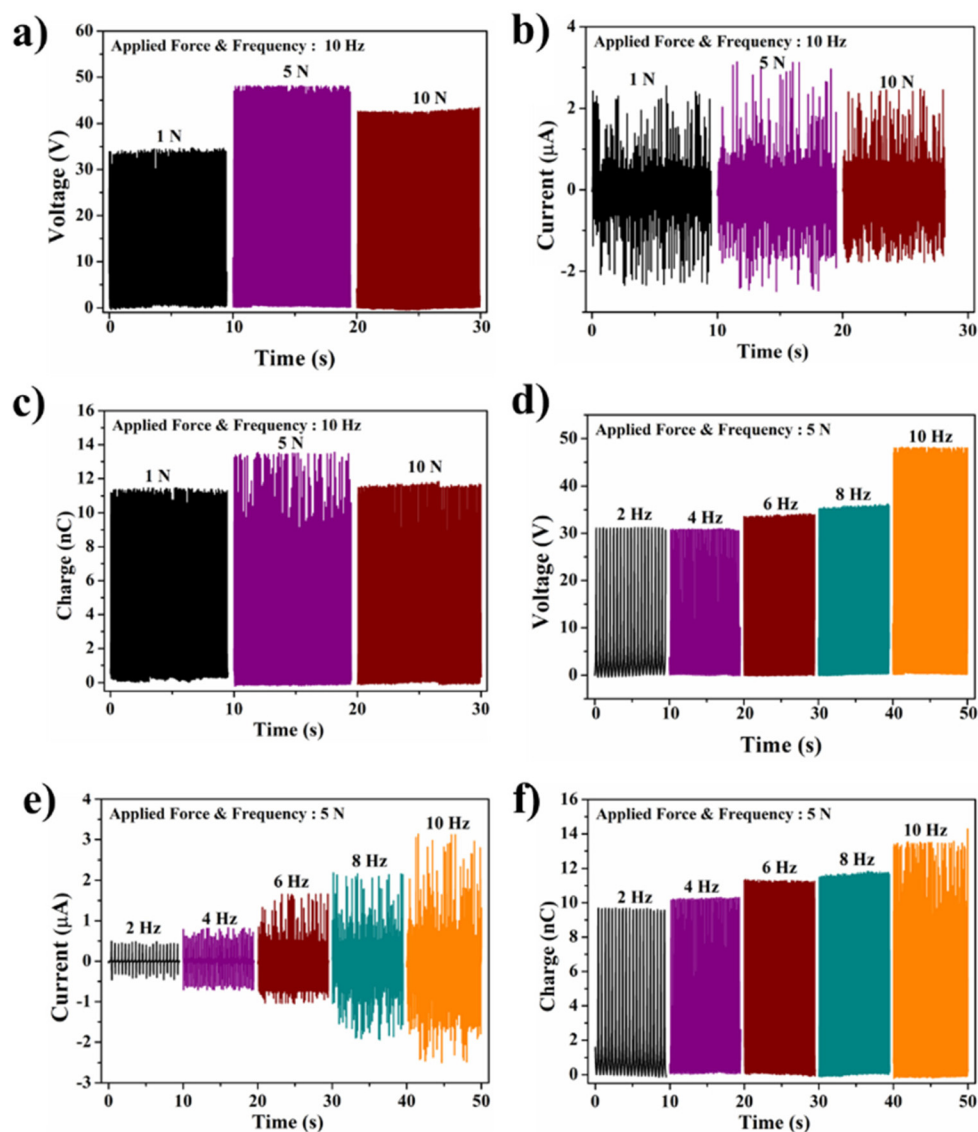
Fig. 6 Triboelectric output on varying the force: (a) V_{oc}, (b) I_{sc} and (c) transferred charge. Triboelectric output on varying the frequency: (d) V_{oc}, (e) I_{sc} and (f) transferred charge.

between 1 N and 10 N while maintaining a constant frequency of 10 Hz. As shown in Fig. 6(a–c), increasing the force from 1 N to 5 N led to an increase in the output voltage, current and charge reaching 48.1 V, 3.1 μA and 13.4 nC for 5 N from 34.4 V, 2.2 μA and 11.7 nC for 1 N force. However, when the force was further increased to 10 N, the output declined to 42.4 V, 2.3 μA and 11.3 nC. The reduction in performance may be attributed to the deterioration of surface microstructures creating a smooth surface, which diminishes the effective contact area and weakens the interaction between triboelectric contact materials.[38] Additionally, excessive force may hinder charge mobility on the surface, potentially causing charge recombination and consequently reducing the overall triboelectric output.

The influence of excitation frequency on the triboelectric performance, a key parameter governing charge transport within the device, was investigated under a constant applied force of 5 N. To assess the electrical characteristics of the TENG, the device was subjected to periodic contact and separation cycles at varying frequencies (2, 4, 6, 8 and 10 Hz) and the TENG output is illustrated in Fig. 6(d–f). The results indicated a progressive increase in I_{sc}, V_{oc} and transferred charge, increasing from 30.8 V, 0.3 μA and 9.6 nC at 2 Hz to 47.9 V, 3.1 μA and 13.4 nC at 10 Hz. This trend aligns with the expected operational behaviour of a TENG, where higher excitation frequencies enhance charge accumulation and transfer.[39] Increased contact–separation rates facilitate rapid charging and discharging, reducing the relaxation time and minimizing charge dissipation, ultimately contributing to improved energy conversion efficiency.

The power output of the 1 cm × 1 cm ABS nanofiber sample, optimized for peak triboelectric output performance (ABS electrospun for 4 hours), was evaluated on pairing with
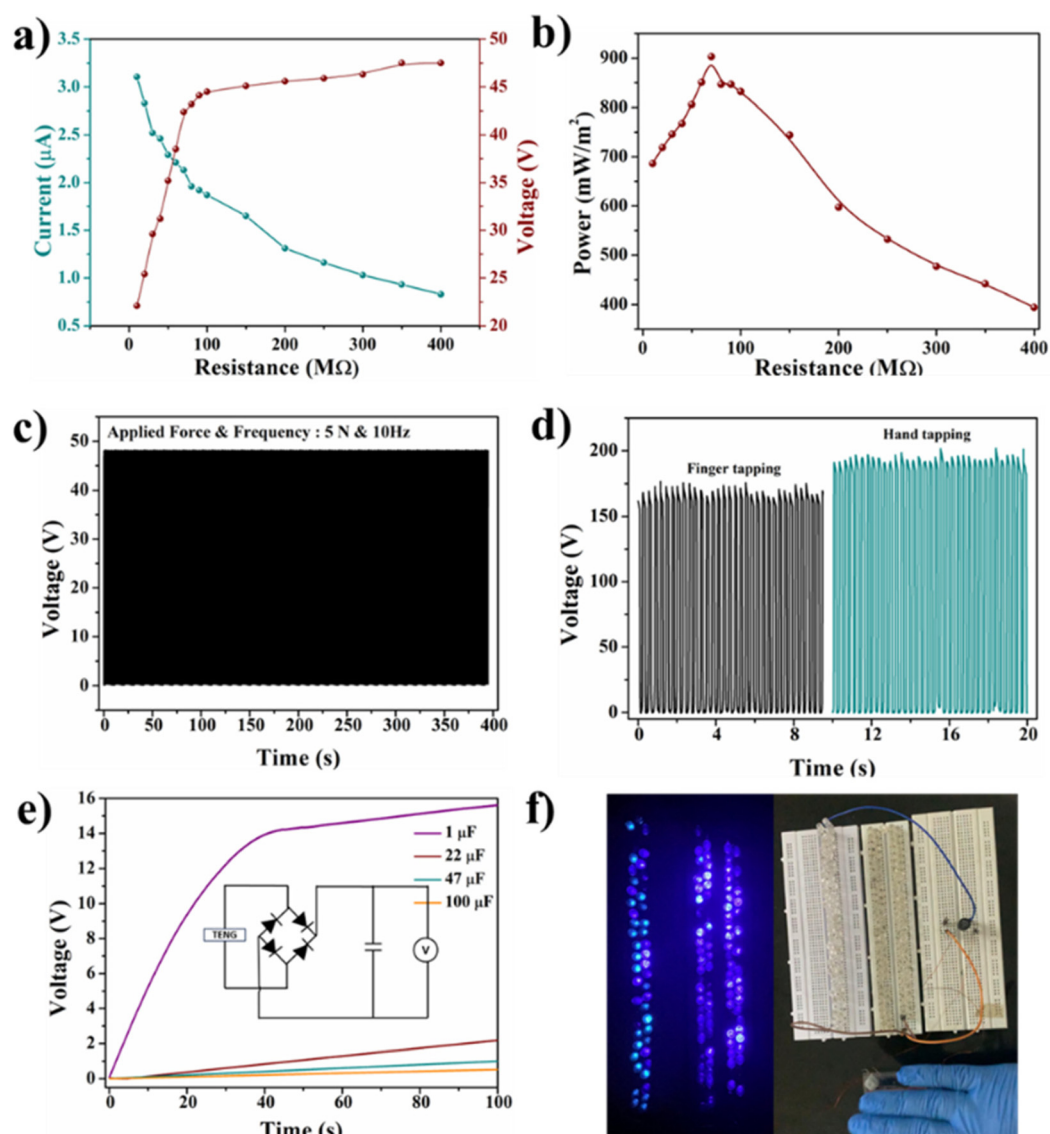
Fig. 7 Electrical measurements on varying the load resistance. (a) V_{oc} and I_{sc}, (b) power output, (c) cyclability study, (d) V_{oc} on finger tapping and hand tapping, (e) charging of commercially available capacitors and (f) powering of LEDs.

FEP. By systematically adjusting the load resistance from 10 MΩ to 400 MΩ, and maintaining the consistent force of 5 N at a frequency of 10 Hz, the resulting triboelectric current and voltage were recorded, as illustrated in Fig. 7(a).

As the resistance increased from 10 MΩ to 400 MΩ, the current decreased from 3.1 μA to 0.8 μA, while the voltage increased from 22.1 V to 47.5 V. The maximum power output was calculated using the product of the highest voltage and current measurements obtained from the resistors, based on the formula $P = VI$. The power density profile, as illustrated in Fig. 7(b), points to the optimal power transfer at 70 MΩ, achieving a power density of 903 mW m^{-2}. This value suggests that the material is a promising candidate for energy harvesting and sensing applications.

The long-term stability of the ABS TENG was tested at 5 N and 10 Hz for 4000 cycles, and it was seen that there was no significant decline in the output voltage, as shown in Fig. 7(c). This indicates its robust mechanical stability, showing its potential as a durable power source for electronic devices. A TENG device was designed to maintain optimal contact and separation on manual hand tapping. For this device, two 4 cm × 4 cm sized copper electrodes were attached to acrylic sheets separated using rubber spacers. The ABS nanofibers were attached to the bottom electrode and FEP was attached to the top electrode using double side tapes. The fabricated TENG showed exceptional efficiency, as the consistent tapping enhanced the interaction between the triboelectric layers, optimizing surface contact and producing a remarkably high electrical output. The electrical performance parameters, such as V_{oc} and I_{sc}, were measured under an applied force range of ~5 N for finger tapping and ~10–12 N for hand tapping and a frequency of ~2–3 Hz, as shown in Fig. 7(d) and Fig. S4a. On

finger tapping, an output of 10 μA and 175 V was observed, which was increased to 12 μA and 200 V on hand tapping. The energy storage performance of the TENG was evaluated by studying its charging and discharging patterns using capacitors with values 1 μF, 22 μF, 47 μF and 100 μF as shown in Fig. 7(e). These capacitors are linked to the TENG while continuous tapping from a human palm was applied. The 1 μF capacitor was charged to 15.6 V on continuous palm tapping for 100 s. Similarly, capacitors of 22 μF, 47 μF and 100 μF were charged to 2.1 V, 1 V and 0.6 V, respectively, on tapping for 100 s. The ABS TENG can light up 166 LEDs instantaneously on continuous tapping, as shown in Fig. 7(f) and Video S1, indicating that the developed TENG can power small electronic devices. This validates the ability of the device to generate power under regular cyclic contact and separation. The flexibility of the ABS nanofiber was shown by integrating the nanofibers in a curved TENG with an ~4 cm radius, as depicted in

Fig. S4b. The triboelectric output was measured at a force of 5 N and a frequency of 10 Hz. For an effective contact of 1.5 cm × 1 cm, the TENG device exhibited a stable output of 50 V and 4.7 μA, as shown in Fig. S4c and d.

Wearable helmet application

The fatalities due to traumatic brain injury (TBI) lead to trauma-related death and disability globally. The effect on the human body during mild TBI is influenced by the magnitude and the place of impact of external forces. The gravity and the potential long-term consequences of recurrent small impact at identical cranial locations as shown in Fig. 8(a) are notably significant, which emphasizes the critical need for effective prevention and accurate detection of the impact mechanism. In this work, the flexibility, mechanical strength and inherent power generation capability of the ABS TENG are utilized to develop an intelligent wearable helmet (Fig. 8(b)). The smart
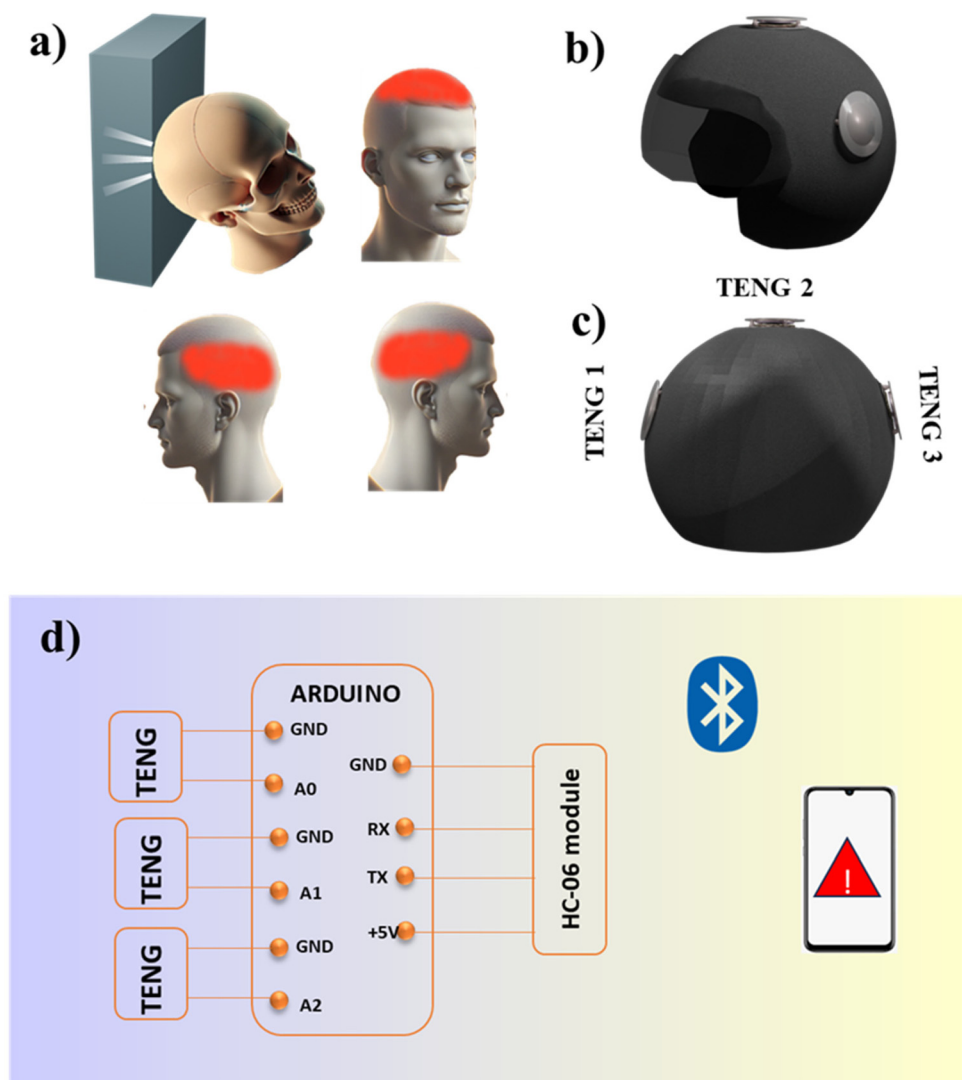

Fig. 8 Design and working of the smart wearable helmet. (a) Schematic representation of the impact on head, (b) schematics of the smart wearable helmet, (c) positioning of the TENG units on the helmet and (d) schematic illustration of the signal transmission circuit.

helmet is designed with a triboelectric module array, a data processing unit and a Bluetooth mobile interface. The helmet features an ABS TENG sensor, measuring 3 cm in diameter and 1 cm in height, as its sensing element, which is positioned on the right, left and top sides of the helmet as shown in Fig. 8(c), to ensure comprehensive spatial coverage and enhanced sensitivity to external impact. The sensors are then linked to a micro-processing module, specifically an Arduino Uno, which serves as the central processing hub for real-time data acquisition and analysis. One electrical lead is inserted into the analog input of the Arduino and the other electrical lead is inserted into the ground terminal. The integration of TENG modules with a microcontroller enables wireless transmission of the data to a mobile terminal, as shown in Fig. 8d. The real-time wireless transmission of the data is achieved using a Bluetooth module HC-06, which can transmit files up to 2.1 Mbps and works on a Bluetooth 2.0 communication protocol. The four pins of the Bluetooth module are connected with the power supply pin (+5), ground pin (GD), receive pin (RX) and transmit pin (TX). (ABS TENG units → Arduino Uno → Bluetooth module HC-06 → mobile phone interface.)

The ABS TENG sensor generates triboelectric voltage signals on the impact of the sensor as a person falls or is subjected to a head impact. These analog signals generated due to the impact on TENG1, TENG2, and TENG3 are fed into the Arduino board *via* the A0, A1 and A3 analog pins as depicted in Fig. 8(d). Data analysis categorizes these signals into head impact at the left side, right side and top side, each producing distinct responses. When an impact is made in the sensor located at the left side, the microcontroller registers the signal and activates the Bluetooth module to send an impact alert to the mobile phone. Similarly, an impact at the right side and top side triggers the microcontroller unit to send the impact alerts to the mobile phone through the Bluetooth module. This activation initiates the transmission of a signal to a paired mobile device, facilitating immediate notification and enabling timely user intervention. The Bluetooth module ensures seamless communication between the helmet and the mobile device, providing a reliable and efficient method for alerting users or emergency contacts in the event of an incident. A video of an individual testing the smart helmet by mimicking an impact, illustrating the pathway of signal transmission, is shown in Video S2. Interfacing the fabricated TENG unit with a microcontroller and Bluetooth module represents a significant advancement in wearable safety technology, offering a robust solution for impact detection and emergency notification in real-world scenarios.

Conclusions

In conclusion, this study fabricated, designed and evaluated an electrospun ABS-based TENG for integration into intelligent wearable helmets. The electrospinning process was optimized to produce neat ABS nanofibers with the highest triboelectric properties in a 37 wt% ABS solution. A TENG unit of 1 cm^2 was fabricated and the triboelectric output was measured at an applied force of 5 N and a frequency of 10 Hz for an ABS nanofiber sample electrospun for 2 h, 4 h, 6 h and 8 h durations. The TENG device showed exceptional triboelectric output with values of 48.1 V, 3.1 μA and 13.4 nC for the sample with a 4 h spinning duration. The effect of force and frequency was systematically studied and the highest efficiency was observed for the sample at 5 N and 10 Hz. The developed TENG with the small size achieved a peak power density of 903 mW m^{-2} at a load resistance of 70 MΩ, highlighting its potential for energy harvesting and sensing. The device operated consistently for over 4000 cycles, maintaining a stable performance. The energy harvesting ability was presented by lighting up 166 blue LEDs and charging commercially available capacitors. The ABS-based TENG was integrated into a helmet to show its practical application in impact detection and real-time alert systems. The TENG units were positioned on different sides of the helmet to absorb the maximum impact. A microcontroller was used to process the analog signal to transmit it through the Bluetooth module, which provided immediate detection and direct user action. This innovative design can be used as an effective impact detection system in industrial, athletics and automotive safety applications, owing to its lightweight, flexible and scalable fabrication technique.

Author contributions

Mathew Sunil: writing – original draft, methodology, investigation, formal analysis and conceptualization; Rinku Thomas: writing – review and editing; K. J. Saji: supervision, methodology and formal analysis; E. J. Jelmy: writing – review &editing; and Honey John: writing – review & editing, supervision, resources, methodology, formal analysis and conceptualization.

Conflicts of interest

There are no conflicts to declare.

Data availability

The authors confirm that the data supporting the findings of this study are available within the article and its supplementary information (SI). Supplementary information is available. See DOI: **https://doi.org/10.1039/d5lp00089k**.

It will also be shared on request.

Acknowledgements

References

1 Z. Li, H. Huang, J. Shen, Y. Gao, X. Zhou, Y. Qian, G. Wang, K. Dong and L. Lyu, *Nano Energy*, 2025, **135**, 110622.

2 P. Parashar, M. K. Sharma, B. K. Nahak, A. Khan, W. Z. Hsu, Y. H. Tseng, J. R. Chowdhury, Y. H. Huang, J. C. Liao, F. C. Kao and Z. H. Lin, *J. Mater. Chem. A*, 2025, **13**, 13750–13762.

3 L. Liu, T. Hu, X. Zhao, Y. Su, D. Yin, C. Lee and Z. L. Wang, *Nano Energy*, 2025, **133**, 110491.

4 S. Kim, Y. Heo, H. Jung, J. Yoo, J.-T. Kim and Y. Park, *Compos. Sci. Technol.*, 2025, **260**, 110985.

5 J. Xu, Z. Wang, H. Y. Nie, Y. Wei and Y. Liu, *Adv. Intell. Syst.*, 2024, **6**, 2300792.

6 T. Eldemerdash, R. Abdulla, V. Jayapal, C. Nataraj and M. K. Abbas, *Adv. Sci. Technol.*, 2020, **29**, 373–387.

7 T. Cheng, J. Shao and Z. L. Wang, *Nat. Rev. Methods Primers*, 2023, **3**, 39.

8 Z. L. Wang, *Adv. Energy Mater.*, 2020, **10**, 2000137.

9 Z. L. Wang and A. C. Wang, *Mater. Today Commun.*, 2019, **30**, 34–51.

10 S. Niu and Z. L. Wang, *Nano Energy*, 2015, **14**, 161–192.

11 J. Luo and Z. L. Wang, *EcoMat*, 2020, **2**, e12059.

12 H. Zou, Y. Zhang, L. Guo, P. Wang, X. He, G. Dai, H. Zheng, C. Chen, A. C. Wang and C. Xu, *Nat. Commun.*, 2019, **10**, 1427.

13 C. Li, Y. Bai, J. Shao, H. Meng and Z. Li, *Small Methods*, 2024, **8**, 2301682.

14 S. A. Lone, K. C. Lim, K. Kaswan, S. Chatterjee, K.-P. Fan, D. Choi, S. Lee, H. Zhang, J. Cheng and Z.-H. Lin, *Nano Energy*, 2022, **99**, 107318.

15 Y. S. Choi, S. W. Kim and S. Kar-Narayan, *Adv. Energy Mater.*, 2021, **11**, 2003802.

16 S. Masihi, M. Panahi, D. Maddipatla, A. J. Hanson, A. K. Bose, S. Hajian, V. Palaniappan, B. B. Narakathu, B. J. Bazuin and M. Z. Atashbar, *ACS Sens.*, 2021, **6**, 938–949.

17 R. Pal, L. Bourgeois, M. Weyland, A. K. Sikder, K. Saito, A. M. Funston and J. R. Bellare, *ACS Omega*, 2021, **6**, 23934–23942.

18 R. Zhang and H. Olin, *EcoMat*, 2020, **2**, e12062.

19 C. Protection, *ABS: Understanding: Impact Resistance and Durability in Protective Gear*, 2023, **https://www.cgprotection.com/news/p_1634.html** (accessed March 4, 2025).

20 N. R. Patra, S. K. Sethi, R. Garg, A. R. Goel, Y. S. Negi and K. Parida, *Nano Energy*, 2024, **130**, 110168.

21 C. Cao, Z. Li, F. Shen, Q. Zhang, Y. Gong, H. Guo, Y. Peng and Z. L. Wang, *Energy Environ. Sci.*, 2024, **17**, 885–924.

22 M. Ibrahim, J. Jiang, Z. Wen and X. Sun, *Nanoenergy Adv.*, 2021, **1**, 58–80.

23 S. Jiang, H. Schmalz, S. Agarwal and A. Greiner, *Adv. Fiber Mater.*, 2020, **2**, 34–43.

24 D. Tao, P. Su, A. Chen, D. Gu, M. Eginligil and W. Huang, *Flexible Electron.*, 2025, **9**, 4.

25 M. Sunil, E. J. Jelmy, K. V. Vijoy, K. J. Saji and H. John, *Sens. Actuators, A*, 2023, **363**, 114730.

26 K. V. Vijoy, H. John and K. J. Saji, *Sustain. Energy Technol. Assess.*, 2023, **58**, 103349.

27 E. Jelmy, D. Jose, K. Vijoy, K. Saji and H. John, *Mater. Adv.*, 2022, **3**, 6897–6907.

28 Y. Liu, J. Mo, Q. Fu, Y. Lu, N. Zhang, S. Wang and S. Nie, *Adv. Funct. Mater.*, 2020, **30**, 2004714.

29 H. Guo, Z. Wen, Y. Zi, M. H. Yeh, J. Wang, L. Zhu, C. Hu and Z. L. Wang, *Adv. Energy Mater.*, 2016, **6**, 1501593.

30 Y. Zheng, N. Meng and B. Xin, *Polymers*, 2018, **10**, 842.

31 J. Xi, S. Shahab and R. Mirzaeifar, *RSC Adv.*, 2022, **12**, 29162–29169.

32 M. Sunil, A. Ramakrishnan, K. Saji and H. John, *Mater. Today Commun.*, 2025, **42**, 111227.

33 X. Kang, C. Pan, Y. Chen and X. Pu, *RSC Adv.*, 2020, **10**, 17752–17759.

34 A. A. Maamoun, A. A. Mahmoud, D. M. Naeim, M. Arafa and A. M. Esawi, *Mater. Adv.*, 2024, **5**, 6132–6144.

35 Y. Dai, X. Zhong, T. Xu, Y. Li, Y. Xiong and S. Zhang, *Energy Technol.*, 2023, **11**, 2300426.

36 Z. Li, M. Zhu, Q. Qiu, J. Yu and B. Ding, *Nano Energy*, 2018, **53**, 726–733.

37 C. Li, J. Zhang, J. Han and B. Yao, *Sci. Rep.*, 2021, **11**, 459.

38 M. L. Seol, S. H. Lee, J. W. Han, D. Kim, G. H. Cho and Y. K. Choi, *Nano Energy*, 2015, **17**, 63–71.

39 W. Liu, Z. Wang, G. Wang, G. Liu, J. Chen, X. Pu, Y. Xi, X. Wang, H. Guo and C. Hu, *Nat. Commun.*, 2019, **10**, 1426.